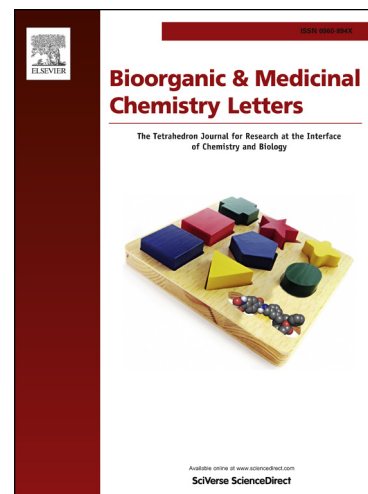


# Accepted Manuscript

## Structure-based Design and Synthesis of Potent Benzothiazole Inhibitors of Interleukin-2 Inducible T Cell Kinase (ITK)

Colin H. MacKinnon, Kevin Lau, Jason D. Burch, Yuan Chen, Jonathon Dines, Xiao Ding, Charles Eigenbrot, Alexander Heifetz, Allan Jaochico, Adam Johnson, Joachim Kraemer, Susanne Kruger, Thomas M. Krülle, Marya Liimatta, Justin Ly, Rosemary Maghames, Christian A.G.N. Montalbetti, Daniel F. Ortwine, Yolanda Pérez-Fuertes, Steven Shia, Daniel B. Stein, Giancarlo Trani, Darshan G. Vaidya, Xiaolu Wang, Steven M. Bromidge, Lawren C. Wu, Zhonghua Pei



PII: S0960-894X(13)01143-8  
DOI: <http://dx.doi.org/10.1016/j.bmcl.2013.09.069>  
Reference: BMCL 20921

To appear in: *Bioorganic & Medicinal Chemistry Letters*

Received Date: 30 July 2013  
Revised Date: 17 September 2013  
Accepted Date: 23 September 2013

Please cite this article as: MacKinnon, C.H., Lau, K., Burch, J.D., Chen, Y., Dines, J., Ding, X., Eigenbrot, C., Heifetz, A., Jaochico, A., Johnson, A., Kraemer, J., Kruger, S., Krülle, T.M., Liimatta, M., Ly, J., Maghames, R., Montalbetti, C.A.G., Ortwine, D.F., Pérez-Fuertes, Y., Shia, S., Stein, D.B., Trani, G., Vaidya, D.G., Wang, X., Bromidge, S.M., Wu, L.C., Pei, Z., Structure-based Design and Synthesis of Potent Benzothiazole Inhibitors of Interleukin-2 Inducible T Cell Kinase (ITK), *Bioorganic & Medicinal Chemistry Letters* (2013), doi: <http://dx.doi.org/10.1016/j.bmcl.2013.09.069>

This is a PDF file of an unedited manuscript that has been accepted for publication. As a service to our customers we are providing this early version of the manuscript. The manuscript will undergo copyediting, typesetting, and review of the resulting proof before it is published in its final form. Please note that during the production process errors may be discovered which could affect the content, and all legal disclaimers that apply to the journal pertain.

## Graphical Abstract

**Structure-based Design and Synthesis of Potent  
Benzothiazole Inhibitors of Interleukin-2 inducible T  
Cell Kinase (ITK)**

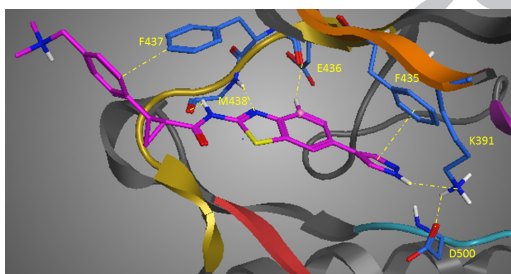
Leave this area blank for abstract info.

Colin H. MacKinnon<sup>a</sup>, Kevin Lau<sup>b</sup>, Jason D. Burch<sup>b</sup>, Yuan Chen<sup>b</sup>, Jonathon Dines<sup>a</sup>, Xiao Ding<sup>b</sup>, Charles Eigenbrot<sup>b</sup>, Alexander Heifetz<sup>a</sup>, Allan Jaochico<sup>b</sup>, Adam Johnson<sup>b</sup>, Joachim Kraemer<sup>c</sup>, Susanne Kruger<sup>c</sup>, Thomas M. Krülle<sup>a</sup>, Marya Liimatta<sup>b</sup>, Justin Ly<sup>b</sup>, Rosemary Maghames<sup>a</sup>, Christian A. G. N. Montalbetti<sup>a</sup>, Daniel F. Ortwine<sup>b</sup>, Yolanda Pérez-Fuertes<sup>a</sup>, Steven Shia<sup>b</sup>, Daniel B. Stein<sup>c</sup>, Giancarlo Trani<sup>a</sup>, Darshan G. Vaidya<sup>a</sup>, Xiaolu Wang<sup>c</sup>, Steven M. Bromidge<sup>a</sup>, Lawren C. Wu<sup>b</sup> and Zhonghua Pei<sup>b,\*</sup>

**13b**ITK  $K_i$  = 0.7 nM

Clp = 12 ml/min

F = 35%





## Structure-based Design and Synthesis of Potent Benzothiazole Inhibitors of Interleukin-2 Inducible T Cell Kinase (ITK)

Colin H. MacKinnon<sup>a</sup>, Kevin Lau<sup>b</sup>, Jason D. Burch<sup>b</sup>, Yuan Chen<sup>b</sup>, Jonathon Dines<sup>a</sup>, Xiao Ding<sup>b</sup>, Charles Eigenbrot<sup>b</sup>, Alexander Heifetz<sup>a</sup>, Allan Jaochico<sup>b</sup>, Adam Johnson<sup>b</sup>, Joachim Kraemer<sup>c</sup>, Susanne Kruger<sup>c</sup>, Thomas M. Krülle<sup>a</sup>, Marya Liimatta<sup>b</sup>, Justin Ly<sup>b</sup>, Rosemary Maghames<sup>a</sup>, Christian A. G. N. Montalbetti<sup>a</sup>, Daniel F. Ortwine<sup>b</sup>, Yolanda Pérez-Fuertes<sup>a</sup>, Steven Shia<sup>b</sup>, Daniel B. Stein<sup>c</sup>, Giancarlo Trani<sup>a</sup>, Darshan G. Vaidya<sup>a</sup>, Xiaolu Wang<sup>c</sup>, Steven M. Bromidge<sup>a</sup>, Lawren C. Wu<sup>b</sup> and Zhonghua Pei<sup>b,\*</sup>

<sup>a</sup>Evotec (UK) Ltd., 114 Milton Park, Abingdon, Oxfordshire, OX14 4SA, United Kingdom

<sup>b</sup>Genentech Inc., 1 DNA Way, South San Francisco, CA 94080, United States

<sup>c</sup>Evotec AG, Manfred Eigen Campus, Essener Bogen 7, D-22419, Hamburg, Germany

### ARTICLE INFO

#### Article history:

Received

Revised

Accepted

Available online

#### Keywords:

ITK inhibitor;

TCR signalling;

Benzothiazole;

Anti-inflammatory;

Asthma

SAR

### ABSTRACT

Inhibition of the non-receptor tyrosine kinase ITK, a component of the T-cell receptor signalling cascade, may represent a novel treatment for allergic asthma. Here we report the structure-based optimization of a series of benzothiazole amides that demonstrate sub-nanomolar inhibitory potency against ITK with good cellular activity and kinase selectivity. We also elucidate the binding mode of these inhibitors by solving the X-ray crystal structures of several inhibitor-ITK complexes.

2012 Elsevier Ltd. All rights reserved.

\* Corresponding author. Tel.: 1-650-467-1542; e-mail: [pei.zhonghua@gene.com](mailto:pei.zhonghua@gene.com)

Interleukin-2 inducible T-cell kinase (ITK), a member of the Tec kinase family of non-receptor tyrosine kinases, plays a major role in T-cell signaling.<sup>1</sup> Along with other T-cell specific tyrosine kinases (including LCK and ZAP-70), ITK serves to amplify the signal associated with the T-cell receptor (TCR) cascade. Aberrant signaling behavior in this cascade is known to lead to autoimmune disorders and inflammation.<sup>2</sup> In studies with ITK knockout mice, levels of Th2 cytokines such as IL-4, IL-5 and IL-13 have been reduced.<sup>3</sup> Moreover, in such mice, the immunological symptoms of allergic asthma were attenuated. Additionally, lung inflammation, eosinophil infiltration and mucous production were drastically reduced in response to challenge with the allergen ovalbumin.<sup>4</sup> These and other reports suggest that selective inhibition of ITK may represent a novel therapy for the treatment of asthma.<sup>5</sup>

Herein we report the optimization of a series of benzothiazole amides starting from a HTS hit **1**, resulting in inhibitors with sub-nanomolar biochemical and sub-micromolar cellular potencies. We also elucidate the binding mode of these inhibitors by solving the X-ray crystal structures of the complexes.

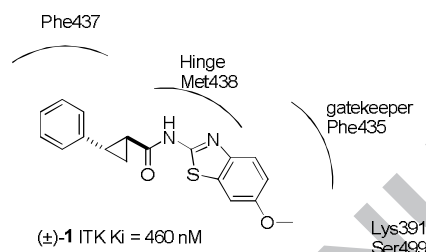
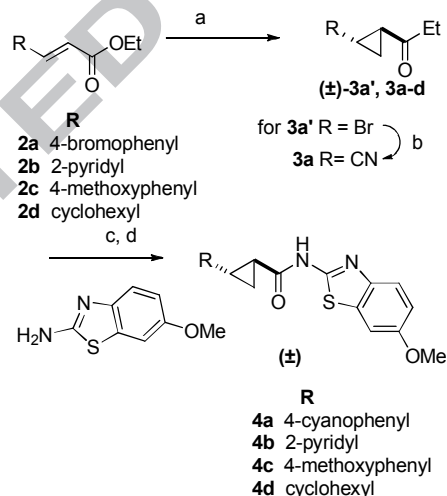


**Figure 1.** Potency and orientation of HTS hit **1** docked in the ATP-binding pocket of ITK.

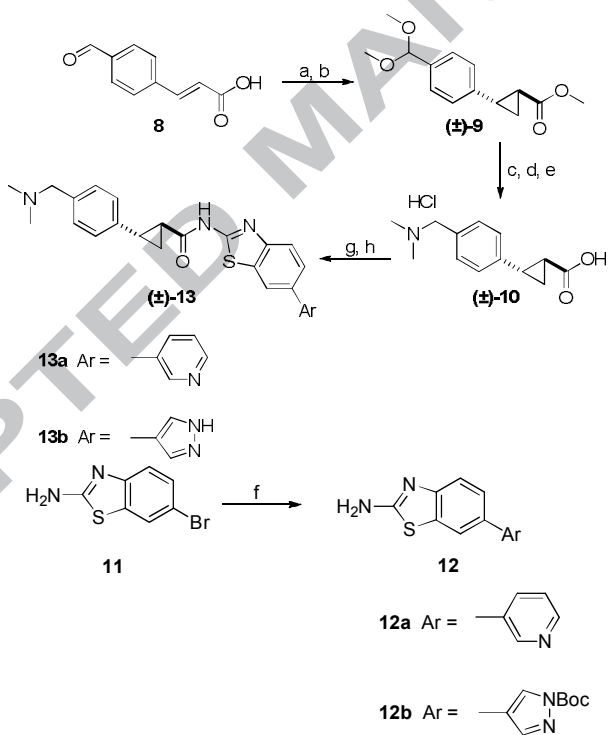
Acid intermediates **3a-d** were obtained from the  $\alpha$ ,  $\beta$ -unsaturated esters **2a-d** by cyclopropanation with the ylide formed from deprotonation of trimethylsulfoxonium iodide by NaH in DMSO to afford esters **3a-d** (Scheme 1).<sup>6,7</sup> In order to synthesize **3a**, the bromine atom was converted to the cyano group in 77% yield. Hydrolysis of the esters afforded the corresponding acids, which were then coupled with the amine to give the desired amides **4a-d**.



**Scheme 1.** Reagents and conditions: (a)  $\text{Me}_3\text{SO}^+\text{I}^-$ , NaH, DMSO, 50 °C, 20-63%; (b) CuCN, DMF, 153 °C, 77%; (c) 2M NaOH, MeOH, 50 °C then 2M HCl (aq), 75-92%; (d) HATU, DIPEA, DMF, 80 °C, 24-71%.

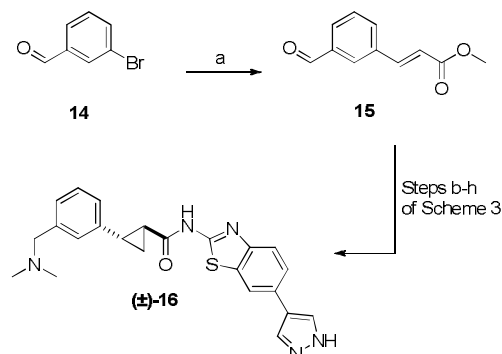
Analogues of 6-heteroaryl benzothiazoles **6a-h** were prepared via Suzuki couplings with commercially available aryl boronic esters or through boronic ester **7** (Scheme 2), both starting from intermediate **5**, itself synthesized according to Scheme 1. Tetrazole **6i** was prepared by cycloaddition of azidotributyl tin and nitrile **5** (R = OMe, X = CN).

Analogs containing basic amines required somewhat more elaborate syntheses. Protection of the aldehyde and ester formation of 4-formyl cinnamic acid **8** in one step using trimethylorthoformate and acetyl chloride in methanol, followed by cyclopropanation provided ester **9** (Scheme 3). Selective deprotection of acetal **9** was achieved by with 2M HCl in methanol and the amino group was installed by standard reductive amination with the resulting aldehyde. Saponification afforded acid **10** which was coupled to benzothiazole aminea **12a-b**, to provide **13a** directly or **13b** after removal of the Boc group. Amines **12a-b** were prepared in one step from commercially available bromide **11** by a Suzuki coupling.

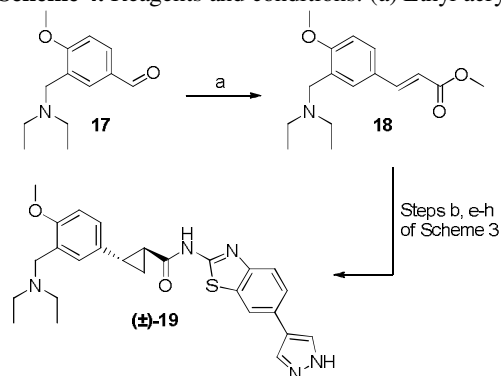


*Meta* isomer **16** was accessed in a similar fashion, where the required cinnamate ester **15** was prepared by a Heck reaction on 3-bromobenzaldehyde **14** (Scheme 4).<sup>8</sup> Finally, trisubstituted benzene analogue **19** was prepared from cinnamic ester **18**, obtained by Horner-Wadsworth-Emmons olefination of the commercially available aldehyde **17** (Scheme 5).

All targets were initially synthesized as racemates. Key compounds, namely **6f**, **13** and **19**, were subsequently resolved using supercritical fluid chromatography (SFC) on a chiral stationary phase.



**Scheme 4.** Reagents and conditions: (a) Ethyl acrylate, Pd(OAc)<sub>2</sub>, NaHCO<sub>3</sub>, Et<sub>3</sub>N, PPh<sub>3</sub>, DMF, 100 °C, 52%.

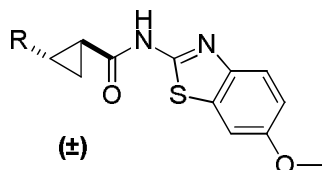


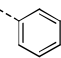
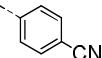
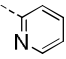
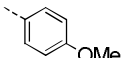
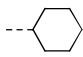
**Scheme 5.** Reagents and conditions: (a) MeO<sub>2</sub>CCH<sub>2</sub>P(O)(OMe)<sub>2</sub>, NaH, THF, rt, quant.

High-throughput screening (HTS) of the Genentech compound library identified racemic benzothiazole amide **1** as a moderately potent inhibitor of ITK (Figure 1). Molecular modeling of **1** bound in the ATP-binding pocket of ITK based on a published ITK crystal structure<sup>9</sup> was used to generate a binding hypothesis (Figure 1). In the model, two hydrogen bonds are formed between the hinge residue Met438 and the two nitrogen atoms of the benzothiazole amide. The cyclopropyl moiety directs the attached benzene ring to achieve a  $\pi$ - $\pi$  interaction with Phe437.

Based on the hypothesized binding mode, we first did a quick survey of the left-hand substitution (LHS). When the phenyl ring was substituted with an electron-withdrawing cyano group, the resulting compound **4a** had potency similar to that of **1** (Table 1).<sup>10</sup> When the phenyl group was replaced with a 2-pyridyl group, the resulting compound **4b** displayed decreased potency. When an electron-donating methoxy group was introduced, the resulting analog **4c** maintained potency, but more importantly the aqueous solubility at pH 7.4 improved from < 2  $\mu$ M of **1** to 11  $\mu$ M. Attempts to reduce planarity by replacing the phenyl group with a cyclohexyl group resulted in significant reduction of potency (**4d**). The above SAR is consistent with the hypothesis that the LHS phenyl ring is engaged in a  $\pi$ - $\pi$  interaction with Phe437.

**Table 1.** LHS SAR of benzothiazole amides

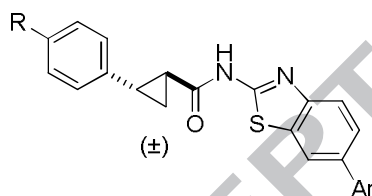


Compound	R	ITK Ki (nM)
<b>1</b>		460
<b>4a</b>		380
<b>4b</b>		2,000
<b>4c</b>		230
<b>4d</b>		3,500

Since the benzothiazole moiety is in the vicinity of the gatekeeper Phe435 according to our binding model, it was envisioned that an aromatic ring attached to C6 position could potentially engage in a  $\pi$ - $\pi$  interaction with this residue. When a 3- or 4-pyridyl group was introduced, the resulting compounds **6a** and **6b** had indeed improved potency while a 2-pyridyl group (**6c**) displayed decreased potency compared to **1** (Table 2), presumably because the polar nitrogen atom has to fit in an hydrophobic pocket. A hydroxymethyl group on the pyridine was introduced to interact with the vicinal Ser499 that is unique to ITK. The resulting analog **6d** displayed improved potency compared to the unsubstituted pyridine analog **6b**. Pyridone **6e**, which was designed to pick up hydrogen-bond interactions with adjacent lysine and aspartic acid residues, also showed improved potency. **6d** and **6e** were the first analogs to achieve Ki < 10 nM.

We then investigated smaller 5-membered aromatic rings attached to the C6 position of the benzothiazole ring. The resulting analog **6f** showed a potency of 6.4 nM. Inhibitory potency decreased when either the pyrazole nitrogen (**6g**) or the adjacent carbon (**6h**) was methylated. Analog **6i** with an acidic tetrazole moiety, designed to interact the nearby Lys391, displayed markedly reduced potency, perhaps because the tetrazole is deprotonated at physiological pH.

**Table 2.** Biochemical and cellular potency of C6-substituted benzothiazole amides



Compound	Ar	R	ITK Ki (μM)	pPLC-γ1 IC <sub>50</sub> (μM)
6a		H	0.050	>20
6b		H	0.085	>20
6c		H	3.5	>20
6d		OMe	0.0053	>20
6e		OMe	0.0066	>20
6f		OMe	0.0064	>14
6g		OMe	0.043	>20
6h		OMe	0.030	>20
6i		OMe	1.1	nd

All compounds summarized in Tables 1 and 2 demonstrated little or no cellular potency, as measured by the inhibition of phosphorylation of ITK's natural substrate phospholipase C-γ1 (PLC γ-1) in Jurkat cells (IC<sub>50</sub> > 14 μM).<sup>11</sup> In addition, the majority of these compounds displayed poor aqueous solubility. In an attempt to address these two issues, we identified the LHS phenyl ring as a promising site to add solubilizing groups in order to improve solubility. A number of analogs with polar substituents on the LHS phenyl group were prepared and tested. From this work, 4-dimethylaminomethyl analogue **13a** (Table 3) displayed ~10-fold potency improvement relative to compound **6b**, so did compound **13b** relative to **6f**. This improved biochemical potency was translated into good cell potency: for example, compound **13b** had a p-PLCγ IC<sub>50</sub> of 89 nM.

A selected number of racemic compounds was resolved by chiral SFC. The (*S, S*) enantiomer was generally more active than its enantiomer. For instance, (*S, S*)-**13b** has a Ki of 0.7 nM, while its enantiomer has a Ki of 6 nM. This is consistent with the binding model as later confirmed by X-ray structure (*vide infra*).

Analogues **16** and **19** with the amine group at the *meta*-position also displayed improved potency compared to **6f** (Table 3). Both compounds displayed improved aqueous solubility compared to **13a** and **13b**, presumably due to reduced symmetry and/or an increased fraction of sp<sup>3</sup> atoms (Fsp<sup>3</sup>, the ratio of sp<sup>3</sup> carbon atoms to total number of carbon atoms). Both strategies are known to disrupt crystal packing and therefore improve solubility.<sup>12</sup> It is worth to note that these optimized inhibitors display from 52-fold (**13a**) to 680-fold (*S, S*)-**6f** selectivity over lymphocyte-specific protein tyrosine kinase (LCK).<sup>13</sup> Because LCK operates upstream of ITK in the TCR cascade and also phosphorylated other Tec family members, inhibition of LCK is expected to affect a broader spectrum of T cells and thus may be undesirable.<sup>13</sup>

**Table 3.** Potency, selectivity and selected physicochemical properties of benzothiazole amides<sup>a</sup>

	ITK Ki (nM)	LCK Ki (μM)	pPLC-γ1 IC <sub>50</sub> (μM)	LogD (pH 7.4)	Solubility <sup>b</sup> (μM)
(±)- <b>6f</b>	6.4	0.89	>14	4.4	<1
( <i>S, S</i> )- <b>6f</b>	2.5	1.7	>20	4.4	<1
(±)- <b>13a</b>	8.4	0.44	10	2.7	<1
(±)- <b>13b</b>	0.6	0.046	0.089	3.0	<1
( <i>S, S</i> )- <b>13b</b>	0.7	0.055	0.091	3.0	<1
(±)- <b>16</b>	1.9	0.15	0.80	2.8	11
( <i>S, S</i> )- <b>19</b>	0.5	0.11	0.048	2.6	180



<sup>a</sup>For structure of **6f**, see Table 2. For structures of **13**, **16** and **19**, see Schemes 3-5. <sup>b</sup> Solubility measured at pH 7.4.

We were able to solve the crystal structures of several inhibitors complexed to ITK as the project progressed. The X-ray crystal structure of **13a** bound to ITK confirmed our hypothesized binding mode (Figure 2a). The nitrogen atom of the benzothiazole and the amide NH form two H-bonds with the backbone NH and the carbonyl of hinge residue Met438, respectively. A non-classical hydrogen bond between the carbonyl group of adjacent residue Glu436 and the hydrogen atom on the C4 of the benzothiazole ring is apparent. The RHS pyridyl ring indeed occupies the nearby pocket and lies underneath gatekeeper Phe435 to form a face-to-face  $\pi$ - $\pi$  interaction. Furthermore, the salt bridge normally observed between the conserved Lys391 and Asp500 residues (*vide infra*) is disrupted due to the movement of the side-chain of Lys391 in order for it to avoid a steric clash with the pyridyl ring of the ligand.

Co-crystallization of **13b** with the kinase domain of ITK was solved to 2.1 Å resolution (Figure 2b). The overall binding mode is very similar to that of **13a**. However, the pyrazole NH now forms a hydrogen bond with the side chain of Lys391 in addition to displaying a  $\pi$ - $\pi$  stacking interaction with the gatekeeper Phe435. This explains why the corresponding N-methylated analog **6g** is less potent, where the H-bond is impossible. This smaller pyrazole ring is well accommodated such that the salt bridge between the conserved Lys391 and Asp500 residues is maintained. These factors combined may explain why 5-membered analog **13b** is about 12-fold more potent than the corresponding 6-membered analog **13a**. The LHS phenyl group is well resolved in this complex, and is shown to be engaged in an edge-to-face  $\pi$ - $\pi$  interaction with Phe437.

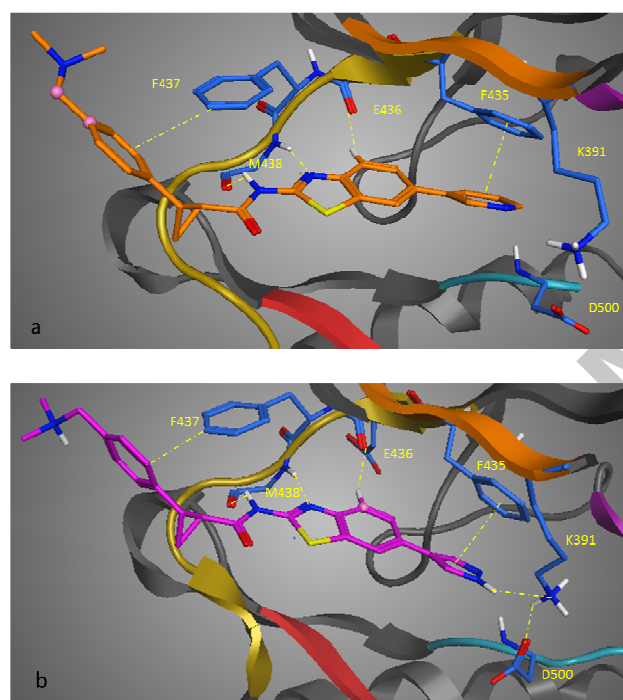


**Figure 2.** X-ray crystal structures of ITK kinase domain complexed with (a) **13a** and (b) (*S,S*)-**13b**. Ligands are shown as ball-and-stick while protein residues are shown in stick. Nitrogen atoms of ITK are in blue, oxygen in red. Only selected residues of ITK are shown for clarity. Interactions between ligand and ITK are indicated by the dashed lines in gold. PDB codes are 4MF0 and 4MF1 for **13a** and **13b**, respectively.

With the single enantiomer of **13b** in hand, we determined its PK profile in rat (Table 4) and were pleased to observe a low clearance (about 20% of hepatic blood flow), acceptable oral bioavailability ( $F=35\%$ ) and a half-life of about 3h. Presumably partial protonation of the weakly basic amine at gastric pH helps solubilize the compound and thus absorption *in vivo*. Compound **13b** also has a low-to-moderate clearance in human hepatocytes of 8.6 ml/min/kg.

**Table 4.** Rat pharmacokinetic profile of amine (*S,S*)-**13b**

Route	Dose	AUC last (h* $\mu$ M)	F (%)	CL (ml/min /kg)	T1/2 (h)	Vss (L/kg)
IV	1 mpk	2.8	NA	12	3.4	3.2

PO 5mpk 4.8 35 NA 3.0 NA

These optimized inhibitors generally demonstrate fair to good kinase selectivity. For instance, only three off-target kinases [Abl, Musk and RAF (Y340D, Y341D)] of the 65 tested, were inhibited >50% by hydroxypyridine **6d** at 1  $\mu$ M.<sup>14</sup> When (*S, S*)-**13b** was tested in the same panel at 0.1  $\mu$ M, eight off-target kinases were inhibited with >50% (Abl, CDK2, CK1 $\alpha$ , Flt3, KDR, PAK4, Txk, YES). We believe that **6d** is more selective than **13b** because of interaction between the hydroxyl group of **6d** and the unique Ser442 of ITK.

In summary, we have discovered a new class of benzothiazole-based ITK inhibitors and were able to improve the potency by 920-fold from a HTS hit through rational design. We were able to elucidate the binding mode of these inhibitors by solving the X-ray crystal structures of representative analogs complexed to the kinase domain of ITK. Advanced leads such as **13b** and (*S, S*)-**19**, possesses sub-nanomolar inhibitory potency, double-digit nanomolar cell potency, triple-digit micromolar aqueous solubility and good selectivity over LCK.

## References & Notes

1. Felices, M.; Falk, M.; Kosaka, Y.; Berg, L.J. *Adv. Immunol.* **2007**, *93*, 145.
2. Sakaguchi, S.; Benham, H.; Cope, A.P.; Thomas R.; *Immunol. Cell Biol.*; **2012**, *90*, 277
3. Mueller, C.; August, A. *J. Immunol.* **2003**, *170*, 5056.
4. Schaeffer, E. M.; Debnath, J.; Yap, G.; McVicar, D.; Liao, X. C.; Littman, D. R.; Sher, A.; Varmus, H. E.; Lenardo, M. J.; Schwartzberg, P. L. *Science* **1999**, *284*, 638.
5. For small-molecule inhibitors of ITK, see (a) Das, J.; Liu, C.; Moquin, R.V.; Lin, J.; Furch, J. A.; Spergel, S. H.; McIntyre, K. W.; Shuster, D. J.; O'Day, K. D.; Penhallow, B.; Huang, C.-Y.; Kanner, S. B.; Lin, T.-A.; Dodd, J. H.; Barrish, J. C.; Wityak, J. *Bioorg. Med. Chem. Lett.* **2006**, *16*, 2411; (b) Lin, T. A.; McIntyre, K.; Das, J.; Liu, C.; O'Day, K. D.; Penhallow, B.; Huang, C.-Y.; Whitney, G. S.; Shuster, D. J.; Xia, X.; Townsend, R.; Postelnik, J.; Spergel, S. H.; Lin, J.; Moquin, R. V.; Furch, J. A.; Kamath, A. V.; Zhang, H.; Marathe, P. H.; Perez-Villar, J. J.; Doweyko, A.; Killar, L.; Dodd, J. H.; Barrish, J. C.; Wityak, J.; Kanner, S. B. *Biochem.* **2004**, *43*, 11056; (c) Snow, R.J.; Abeywardane, A.; Campbell, S.; Lord, J.; Kashem, M. A.; Khine, H. H.; King, J.; Kowalski, J. A.; Pullen, S. S.; Roma, T.; Roth, G. P.; Sarko, C. R.; Wilson, N. S.; Winter, M. P.; Wolak, J. P.; Cywin, C. L. *Bioorg. Med. Chem. Lett.* **2007**, *17*, 3660; (d) Moriarty, K. J.; Winters M, Qiao, L.; Ryan, D.; Desjarlis, R.; Robinson, D.; Cook, B. N.; Kashen, M. A.; Kaplita, P. V.; Liu, L. H.; Farrell, T. M.; Khine, H. H.; King, J.; Pullen, S. S.; Roth, G. P.; Magolda, R. Takahashi, H. *Bioorg. Med. Chem. Lett.* **2008**, *18*, 5537; (e) Winters, M.P.; Robinson, D. J.; Khine, H. H.; Pullen, S. S.; Woska Jr.; J. R.; Raymond, E. L.; Sellati, R.; Cywin, C. L.; Snow, R. J.; Kashem, M. A.; Wolak, J. P.; King, J.; Kaplita, P. V.; Liu, L. H.; *Bioorg. Med. Chem. Lett.* **2008**, *18*, 5541; (f) Riether, D.; Zindell, R.; Kowalski A, et al. *Bioorg. Med. Chem. Lett.* **2009**, *19*, 1588; (g) Lo H.Y.; Bentzien, J.; Fleck, R. W.; Pullen, S. S.; Khine, H. H.; Woska, J. R.; Kugler, S. Z.; Kashen, M. A.; Takahashi, H. *Bioorg. Med. Chem. Lett.* **2008**, *18*, 6218; (h) Charrier, J. D.; Miller, A.; Kay, D. P.; Brenchley, G.; Twin, H. C.; Collier, P. N.; Ramaya, S.; Keily, S. B.; Durrant, S. J.; Knegetel, R. M.; Tanner, A. J.; Brown, K.; Curnock, A. P.; Jimenez, J. M. *J. Med. Chem.* **2011**, *54*, 2341; (i) Herdemann, M.; Weber, A.; Jonveaux, J.; Jonveaux, J.; Schwoebel, S.; Heit, I. *Bioorg. Med. Chem. Lett.* **2011**, *21*, 1852; (j) McLean, L. R.; Zhang, Y.; Zaidi, N.; Bi, X.; Wang, R.; Dharanipragada, R.; Jurcak, J. G.; Gillespy, T. A.; Zhao, Z.; Musick, K. Y.; Choi, Y. M.; Barrague, M.; Peppard, J.; Smicker, M.; Duguid, M.; Parker, A.; Fordham, J.; Kominos, D. *Bioorg. Med. Chem. Lett.* **2012**, *22*, 3296; (k) Zapf, C. W.; Gerstenberger, B. S.; Xing, L.; Limburg, D. C.; Anderson, D. R.; Caspers, N.; Han, S.; Aulabaugh, A.; Kurumbail, R.; Shukla, S.; Li, X.; Spaulding, V.; Czerwinski, R. M.; Seth, N.; Medley, Q. G. *J. Med. Chem.*, **2012**, *55*, 10047. (l) For a recent review on ITK inhibitors, see: Charrier, J.-D.; Knegetel, R. MA. *Expert Opin. Drug Discov.* **2013**, *8*, 369.
6. Newcomb, M.; Choi S, Toy, P.H. *Can. J. Chem.* **1999**, *77*, 1123.
7. Hamdouchi, C.; Topolski, M.; Goedkin, V.; Walborsky, H. M. *J. Org. Chem.* **1993**, *58*, 3148.
8. Biedeger, R.J.; Decker, R.E.; Dupre, B.; Hamaker, L.K.; Holland, G.W.; Kassir, J.M.; Li, W.; Market, R.V.; Nguyen, N.; Scott, I. L.; Wu, C. European Patent: EP 1213288 A1, 2002.
9. (a) Brown, K.; Long, J.M.; Vial, S.C.M.; Dedi, N.; Dunster, N.J.; Renwick, S.B.; Tanner, A.J.; Frantz, J.D.; Fleming, M.A.; Cheetham, G.M.T.; J. Biol. Chem. **2004**, *279*, 18727; (b) Kutach, A.K.; Villaseñor, A.G.; Lam, D.; Belunis, C.; Janson, C.; Lok, S.; Hong, L.N.; Liu, C.M.; Deval, J.; Novak, T.J.; Barnett, J.W.; Chu, W.; Shaw, D.; Kuglstatler, A. *Chem. Biol. Drug Des.* **2010**, *76*, 154.
10. Biochemical assay: GST-ITK full length enzyme was from Invitrogen (PV3875) and substrate was BLK peptide (Ac-EFPIYDFLPAKKK-NH<sub>2</sub>). Reactions were carried out in a final volume of 51  $\mu$ l with 50 mM HEPES (pH 7.2), 15 mM MgCl<sub>2</sub>, 2 mM DTT, 0.015% Brij-35, 1 nM ITK, 2  $\mu$ M substrate, 20  $\mu$ M ATP, and 2% DMSO. After 35 min incubation at RT, reactions were stopped upon addition of 10  $\mu$ l of 30% TCA. Samples were centrifuged (4350 rpm, 4 °C, 5 min) and subjected to LC/MS analysis on a Waters Acquity UPLC/TQD system equipped with a Waters Acquity UPLC BEH C18 (2.1  $\times$  50 mm) 1.7  $\mu$ m column (injection volume: 5  $\mu$ l, column temperature: 60 °C, flow rate: 1 ml/min, solvent A: 0.1% formic acid in LC/MS grade water, solvent B: 0.1% formic acid in LC/MS grade ACN). Analytes were separated by applying a gradient from 15 to 32% solvent B within 0.7 min and detected in positive mode ESI-MS/MS by MRM (multiple reaction monitoring) of transitions 819.8/84.8 (BLK substrate) and 859.0/84.8 as well as 859.0/120.7 (phosphorylated BLK product).
11. The ability of compounds to inhibit phosphorylation of PLC $\gamma$ 1 in Jurkat cells was determined using an immuno-detection assay that will be described in detail in a separate communication.
12. Ishikawa, M.; Hashimoto, Y. *J. Med. Chem.* **2011**, *54*, 1539.
13. (a) For a benzothiazole-based LCK inhibitor, see Das, J.; Lin, J.; Moquin, R. V.; Shen, Z.; Spergel, S. H.; Wityak, J.; Doweyko, A. M.; DeFex, H. F.; Fang, Q.; Pang, S.; Pitt, S.; Shen, D. R.; Schieven, G. L.; J. C. Barrish. *Bioorg. Med. Chem. Lett.* **2003**, *13*, 2145; (b) We did not have in-house X-ray crystal structure of LCK, so do not have structure-based explanation of selectivity over LCK.
14. Selectivity screening was performed by SelectScreen® Kinase Profiling Services (Invitrogen-Life Technologies, Madison, USA).

## Graphical Abstract

**Structure-based Design and Synthesis of Potent  
Benzothiazole Inhibitors of Interleukin-2 Inducible T  
Cell Kinase (ITK)**

Leave this area blank for abstract info.

**13b**

ITK  $K_i$  = 0.7 nM

Clp = 12 ml/min

F = 35%

